Plant Biotechnology Journal (2005) **3**, pp. 341–351 doi: 10.1111/j.1467-7652.2005.00128.x

Mutan produced in potato amyloplasts adheres to starch granules

Géraldine A. Kok-Jacon†, Jean-Paul Vincken, Luc C. J. M. Suurs and Richard G. F. Visser*

Graduate School Experimental Plant Sciences, Laboratory of Plant Breeding, Wageningen University, PO Box 386, 6700 AJ Wageningen, The Netherlands

Received 22 October 2004;
revised 22 January 2005;
accepted 25 January 2005.
**Correspondence* (fax +31 (0)317 483457;
e-mail richard.visser@wur.nl)
†*Present address*: Unité de Biochimie Physiologique, Institut des Sciences de la Vie, University of Louvain, Croix du Sud 2-20, B-1348 Louvain-la-Neuve, Belgium

Keywords: adhesiveness, glucan-binding domain, glucansucrase, mutan, transgenic potato, truncation.

Summary

Production of water-insoluble mutan polymers in Kardal potato tubers was investigated after expression of a full-length (*Gtf*I) and a truncated mutansucrase gene referred to as *GtfICAT* (*Gtf*I without glucan-binding domain) from *Streptococcus downei.* Subsequent effects on starch biosynthesis at the molecular and biochemical levels were studied. Expression of the *GtfICAT* gene resulted in the adhesion of mutan material on starch granules, which stained red with erythrosine, and which was hydrolysed by exo-mutanase. In addition, *GtfICAT*-expressing plants exhibited a severely altered tuber phenotype and starch granule morphology in comparison to those expressing the full-length *Gtf*I gene. In spite of that, no structural changes at the starch level were observed. Expression levels of the sucrose-regulated, *AGPase* and *GBSSI* genes were down-regulated in only the GTFICAT transformants, showing that *GtfICAT* expression interfered with the starch biosynthetic pathway. In accordance with the down-regulated *AGPase* gene, a lower starch content was observed in the GTFICAT transformants. Finally, the rheological properties of the GTFICAT starches were modified; they showed a higher retrogradation during cooling of the starch paste.

Introduction

In planta production of bacterial extracellular polysaccharides could generate a resource with unique environmental and commercial added values (Moire *et al*., 2003). For instance, adhesive properties of bacterial polysaccharides such as xanthan and pullulan are actually regarded as possible replacements of synthetic paper and wood adhesives (Haag *et al*., 2004). Another polysaccharide with adhesive properties is mutan (see further). Besides, the *in planta* production of bacterial polymers may alter the properties of existing polymers such as starch, which is of particular interest to us. It could be advantageous to replace post-harvest chemical starch modifications by a more environment-friendly bioprocessing.

Expression of the *Gtf*I mutansucrase gene (Ferretti *et al*., 1987), which is produced by the oral cariogenic *Streptococcus downei* Mfe28 bacteria, leads to the accumulation of mutan polymers in the presence of sucrose. According to *in vitro* experiments, GTFI catalyses the formation of two types of chemical linkages between glucosyl residues, i.e. α-(1 > 3)-linkages (88%), forming the backbone of mutan, and α-(1 > 6) linkages (12%), connecting single unit glucosyl residues to the backbone (Russell *et al*., 1987; Monchois *et al*., 1999b). Mutan polymers account for about 70% of the carbohydrates present in dental plaque (Loesche, 1986), the formation of which is briefly discussed in succeeding discussions. Saliva-coated enamel surfaces are colonised by diverse oral bacteria, referred to as the early colonisers that adhere to receptors present on teeth surfaces by means of adhesin proteins. In turn, these bacteria secrete various polysaccharides such as mutans, dextrans and levans that exhibit different degrees of water-solubility (Sutherland, 2001). These polymers, together with the early colonisers, enhance the aggregation of the late colonisers, creating a biofilm, which is usually named dental plaque (Marsh, 2003). Dental plaque stains red by erythrosine (Leknes and Lie, 1988), an iodine-containing molecule. Iodine is thought to be responsible for binding to the constituent polysaccharides. From the polymers that are formed, mutan is the most adhesive and water-insoluble (Hamada and Slade, 1980). Interestingly, the chain conformation of mutan is very similar to that of cellulose, an extended helix with a two-fold symmetry, which may explain

its poor solubility in water (Marchessault and Deslandes, 1980). The exact adhesion mechanism by which mutans adhere to surfaces in relation to the other dental plaque components requires further elucidation, although there is some evidence that α-(1 > 6)-linked glucosyl residues might contribute to adhesive properties (Colby *et al*., 1999).

Because of their implications in human dental caries, different studies with genetically engineered GTFIs have been carried out in order to elucidate structure-function relationships with respect to mutan synthesis. GTFI, which belongs to family 70 of the glycoside hydrolases (<http://afmb.cnrs-mrs.fr/CAZY/>), has a primary structure, which is common to all glucansucrase enzymes, consisting of a signal peptide, a variable region, a catalytic domain (CAT) and a glucan-binding domain (GBD) (Monchois *et al*., 1999b). Its enzymatic reaction takes place by a so-called two-site insertion mechanism in which glucose residues from sucrose molecules are polymerized in a growing mutan chain, or linked to carbohydrate acceptor molecules (Robyt, 1995). Until now, studies on GTFI acceptor reaction efficiency have not been done. Interestingly, expression of only its catalytic domain resulted in an active GTFI enzyme, with an activity of approximately 70% of the WT enzyme (Monchois *et al*., 1999a). Glucan-binding domains of GTFI share sequence homologies with the glucan-binding protein of *Streptococcus mutans* and the choline-binding domain of pneumococcal proteins (Wren, 1991). As their name implies, their role is to mediate the binding of the synthesized glucan chains to the enzyme. Industrial applications of mutan polymers have not been developed as far as we know. However, they could be of interest as functional food (prebiotics) (Tuohy *et al*., 2003) and possibly as glues.

The aim of this study is to produce mutan polymers in potato amyloplasts by expressing a full-length and a glucan-binding domain-truncated gene. Amyloplastic transport of the truncated enzyme may be enhanced because of its smaller molecular size. Therefore, the truncated and full-length GTFIs are evaluated with respect to their efficiency in mutan production in the amyloplast. In addition, the effects of the introduction of these genes on starch biosynthesis are investigated at the molecular and biochemical levels.

Results

High *GtfICAT* mRNA level correlates with altered tuber phenotype

The plastidic protein-targeting sequence (FD) (Gerrits *et al*., 2001) was fused in frame to the mature or GBD-truncated *Gtf*I genes (Figure 1). These fragments were driven by the patatin promoter allowing high tuber expression (Wenzler *et al*., 1989). For each of the constructs, restriction sites were engineered at the FD▲ gene fusion, creating two mutations (VTAM↓ATYKVTLITK▲DTE became VTAM↓ATYKVTLIT**P**▲**G**TE, in which ↓ represents the splice site for amyloplast entry and ▲ the gene fusion). In addition, the pPFIC sequence differed from the published GTFI sequence (Ferretti *et al*., 1987) at position 408 (L_{408}**F**) which did not affect any conserved residue. Thirty independent transgenic potato clones were obtained after *Agrobacterium*-mediated plant transformation with pPFI and pPFIC. Five plants of each transgenic clone were grown in the greenhouse for tuberization to ensure enough material and the resulting tubers were pooled for further characterization. Transformed potato plant series are referred to as KDIxx and KDICxx, in which I and IC represent the *Gtf*I and *GtfICAT* genes, respectively, and xx the clone number. The untransformed genotype is referred to as KD-UT.

Reverse transcriptase polymerase chain reaction (RT-PCR) was performed on a number of transformants that were divided in classes, based on the band intensity of the different PCR products. The band intensities were compared to that of *Ubi3*, which is used as an internal control (Garbarino and Belknap, 1994). From the KDI series, the KDI14 (–), KDI2 (–), KDI26 (+), KDI30 (+), KDI11 (++) and KDI20 (++) transformants were selected for further characterization (Figure 2A) in which (–) (+) and (++) represent no, intermediate and high levels of mRNA, respectively. Because of the low *Ubi3*

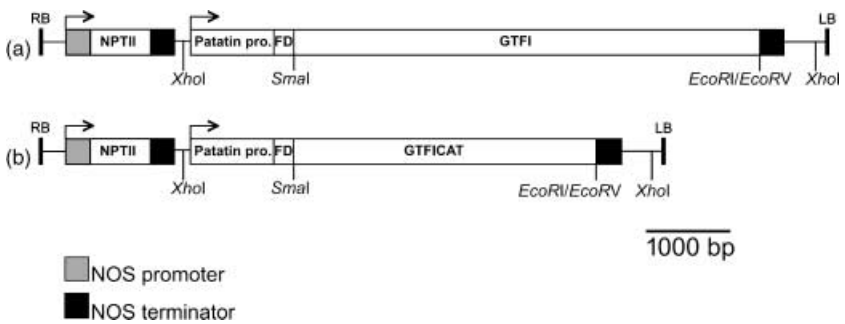

Figure 1 Schematic representation of pPFI (a) and pPFIC (b) binary vectors used for potato plant transformation.

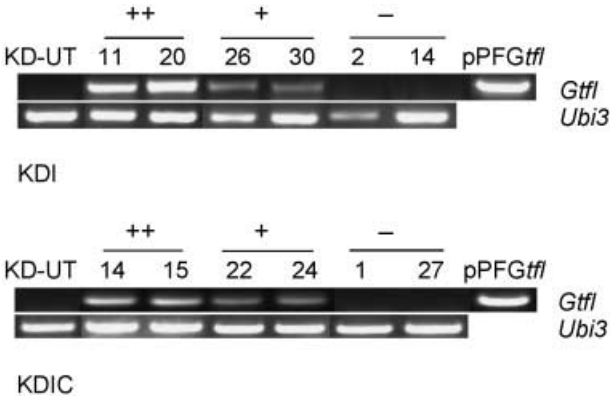

Figure 2 RT-PCR analysis of the selected KDI and KDIC transformants, and KD-UT. The upper panel shows the PCR products using the primers designed on the *Gtf*I and *GtfICAT* sequences from the KDI and KDIC transformants, respectively. The lower panel shows the PCR products using the primers designed on the *Ubi3* sequence that served as an internal control. pPF*Gtfl* plasmid: positive control.

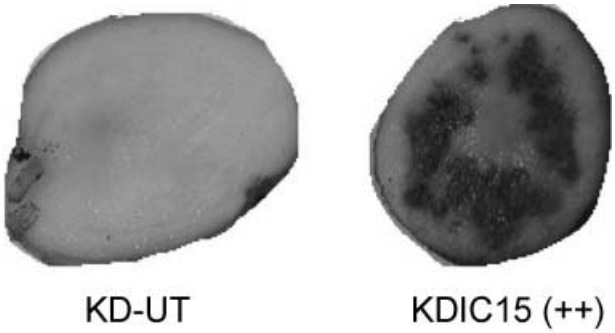

Figure 3 Tuber phenotype of the KDIC15 (++) transformant compared to that of KD-UT.

intensity of KDI2, this transformant might also be attributed to the (+) class. In addition, KDIC1 (–), KDIC27 (–), KDIC22 (+), KDIC24 (+), KDIC14 (++) and KDIC15 (++) transformants were selected from the KDIC series (Figure 2B). As expected, no *Gtf*I mRNA was detected in the KD-UT plants.

A severely altered tuber phenotype was found for the (++) class of the KDIC series in which almost all the tubers exhibited brownish/reddish discoloration (see Figure 3), which was present inside and close to the vascular regions of the tuber. Before starch isolation, each tuber was cut in two parts in order to check the coloration. The (+) class transformants also showed such a phenotype but to a lesser extent (data not shown). The (–) class transformants exhibited a tuber phenotype comparable to KD-UT. Thus, the colour of the tuber tissue seemed to be correlated with the level of *GtfICAT* expression. No phenotypical alterations were observed for the KDI series. For the KDI and KDIC series, the tuber number, yield and plant morphology were unchanged and comparable to KD-UT.

Mutans are only visualized in the (+) and (++) classes of KDIC transformants

An erythrosine red-colouring solution was used for the visualization of mutans attached to starch granules. As a positive control, mutan polymers (Wiater *et al*., 1999) were stained with this colouring agent (Figure 4B); normal starch granules, containing amylopectin and amylose, did not stain with the dye. Interestingly, mutans were present on KDIC15 starch granule surfaces (Figure 4C). A red staining was also observed on KDIC14 and KDIC22 starch granule surfaces, but to a lesser extent (data not shown), but no coloration was observed for the KDI series, which was comparable to KD-UT (Figure 4A). When KDIC15 starch granules were treated with an exo-mutanase solution

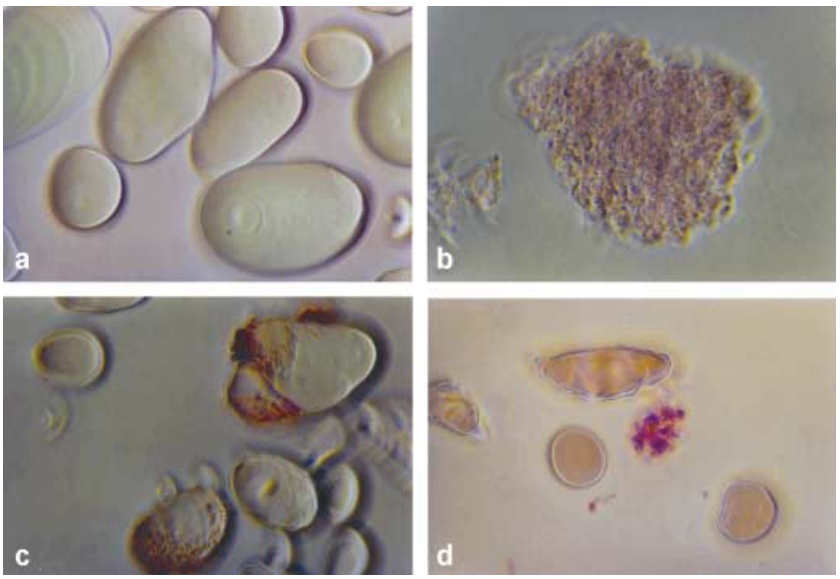

Figure 4 LM analysis of starch granules (× 800) stained with Disclosing solution red-Cote from KD-UT (a) and KDIC15 (c) compared to that of mutan polymers (b). (d) Treatment of KDIC15 starch granules with 25 mU of exo-mutanase enzyme.

(Figure 4D), most of the mutans were detached from the starch granules. This provided additional proof that the red-staining patches on starch granules corresponded to mutan. It also suggests that the binding only occurred at the starch granule surface.

GBD truncation correlates with a severely altered granule morphology

The morphology of starch granules was determined by SEM and LM. With SEM, the presence of altered starch granules was observed for the KDI and KDIC series, particularly for the (++) class (Figure 5: C-D-G-H-J-K-L-M) and (+) class (data not shown) of transformants. The granule morphology of the (–) class (Figure 5: B and F, representing the KDI and KDIC series, respectively) was comparable to that of KD-UT (Figure 5: A-E). For the (++) class of the KDI series, starches contained uncommonly shaped granules with protruded forms and with small granules that associated to larger ones (Figure 5: C-D-J-K). For the (++) class of the KDIC series, starch granules exhibited uncommon shapes with eroded and protruded forms (Figure 5: G-H-L-M). In addition, pores in the granule surface were often observed. With LM, the presence of altered starch granules was confirmed for each of the series, in particular for the (++) and (+) classes (data not shown). It seems that expression of a GBD-truncated *Gtf*I induces a more severe effect on starch granule morphology than the mature one. Quantification of altered starch granules number such as those represented in Figure 5 (J-K-L-M) was performed by analysing a population of 100 starch granules in triplicate for a representative transformant of the (–) and (+) classes and two transformants of the (++) class for each series. This quantification is shown in Figure 6 for the KDI14 (–), KDI30 (+), KDI11 (++), KDI20 (++) and KDIC1 (–), KDIC22 (+), KDIC14 (++), KDIC15 (++) transformants. The highest percentage of

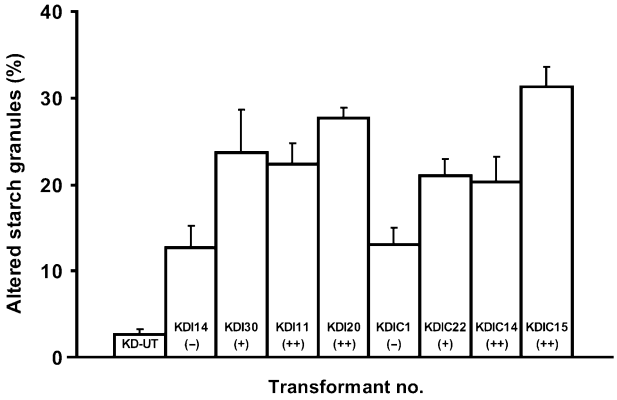

Figure 6 Percentage of starch granules with altered morphology (see Figure 5. j, k, l, m) in selected transformants compared to KD-UT (i).

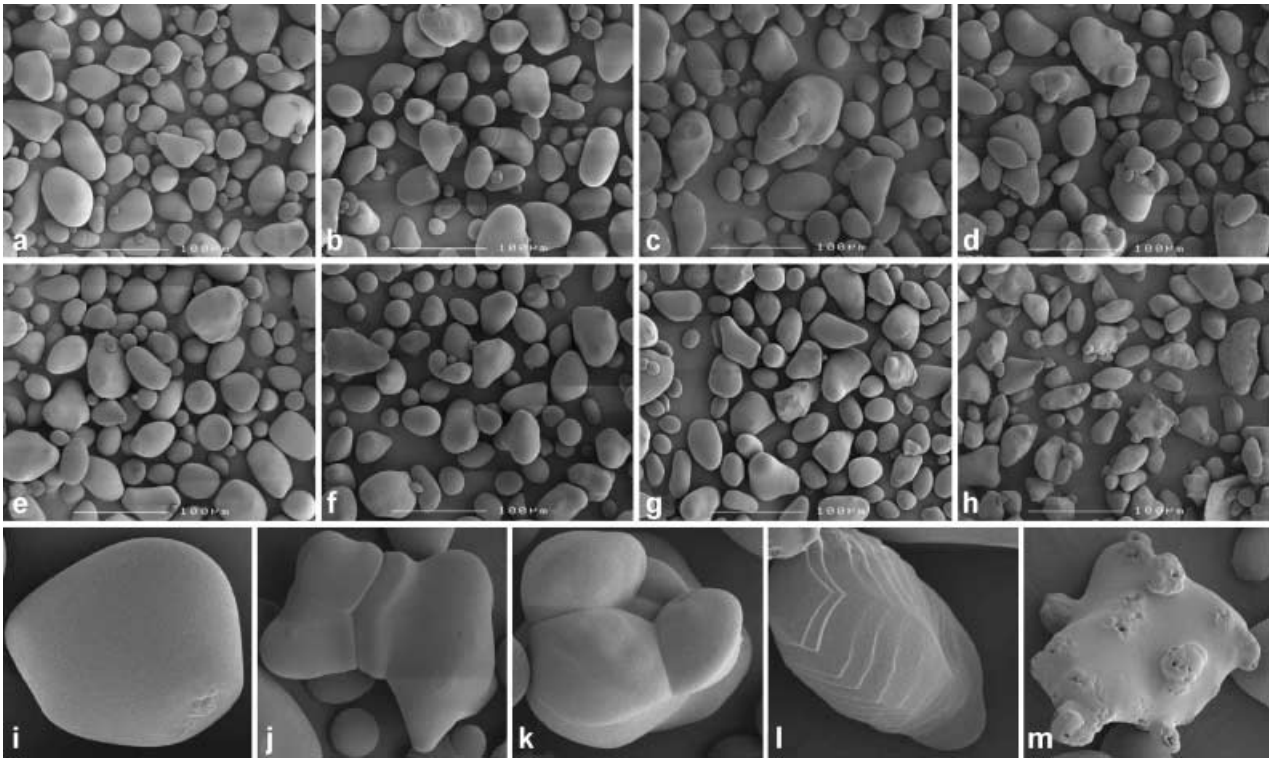

Figure 5 SEM analysis of starch granules (× 350) from KD-UT (a, e) compared to that of selected transformants (KDI14 (b), KDI11 (c), KDI20 (d), KDIC1 (f), KDIC14 (g) and KDIC15 (h)), and examples of starch granules (× 1000) with altered morphology (KDI11 (j), KDI20 (k), KDIC14 (l) and KDIC15 (m)) compared to KD-UT (i).

Table 1 Overview of physicochemical properties and starch content of KDI transformants: Summary of granule size (d_{50}), gelatinization characteristics (T_o, ΔH), amylose and starch content measurements of starches from the selected transformants and KD-UT. Data (± SD) are the average of two or three independent measurements.

Transformants	d_{50} (μM)*	T_o (°C) †	ΔH (kJ/g)‡	Amylose content (%)	Starch content (mg/g FW)
KD-UT	21.5 (± 0.4)	66.6 (± 0.1)	14.3 (± 2.1)	19.5 (± 0.4)	226.4 (± 49.3)
KDI14 (–)	21.8 (± 0.8)	67.0 (± 0.1)	14.4 (± 0.5)	19.4 (± 0.1)	211.5 (± 88.4)
KDI2 (–)	20.3 (± 0.5)	64.7 (± 0.1)	15.7 (± 0.2)	19.5 (± 0.2)	355.6 (± 41.9)
KDI26 (+)	21.9 (± 0.6)	67.1 (± 0.1)	15.5 (± 0.1)	19.2 (± 0.3)	214.7 (± 110.8)
KDI30 (+)	18.6 (± 0.0)	64.8 (± 0.4)	13.0 (± 0.1)	19.3 (± 0.2)	286.0 (± 120.1)
KDI11 (++)	25.1 (± 0.8)	66.3 (± 0.1)	14.4 (± 0.1)	19.1 (± 0.1)	209.7 (± 115.2)
KDI20 (++)	19.6 (± 0.5)	66.0 (± 0.4)	14.2 (± 0.1)	19.1 (± 0.3)	319.3 (± 97.0)

*Median value of the granule size distribution.
†Temperature of onset of starch gelatinization.
‡Enthalpy released.

altered starch granules was found in the (+) and (++) classes of the KDI and KDIC transformants, ranging from 22.3 ± 2.5% for KDI11 to 31.3 ± 2.3% for KDIC15. For the (–) class of transformants, the frequency of altered starch granules was about 13%, and that of KD-UT about 3%.

The (++) KDIC transformants exhibit decreased starch content and novel physicochemical properties

Starch content (Table 2) of the (++) KDIC class was decreased, ranging from 114.5 ± 43.6 mg/g FW for KDIC14 to 81.3 ± 37.3 mg/g FW for KDIC15 in comparison to KD-UT (190.7 ± 15.2 mg/g FW). Starch content of the KDI (Table 1), the (–) and (+) classes of the KDIC transformants (Table 2) was comparable to that of KD-UT.

Median granule size (d_{50}), gelatinization characteristics (T onset (T_o) and enthalpy released (ΔH)) and amylose content (Tables 1 and 2) of the transgenic starches were also determined, and no significant differences were found in comparison to KD-UT. The viscosimetric analysis showed that KDIC15 starch (Figure 7(1)) had different behaviour from that of KDI20 (Figure 7(2)) and KD-UT (Figure 7(3)), particularly with respect to the end viscosity, which was about 1.7-fold higher.

The presence of α-(1 > 3)-linked mutan chains in starch was investigated by treating the gelatinized starches with isoamylase and α-amylase, followed by chromatography of the reaction products. After complete debranching of the starch molecules with isoamylase, we did not observe differences between KD-UT and transgenic starches upon HPSEC, neither shifts in populations of amylopectin side chains, nor the appearance of a new peak which could correspond to mutan. With high-performance anion-exchange chromatography (HPAEC) which gives a better separation of the smaller amylopectin side chains, a similar result was obtained;

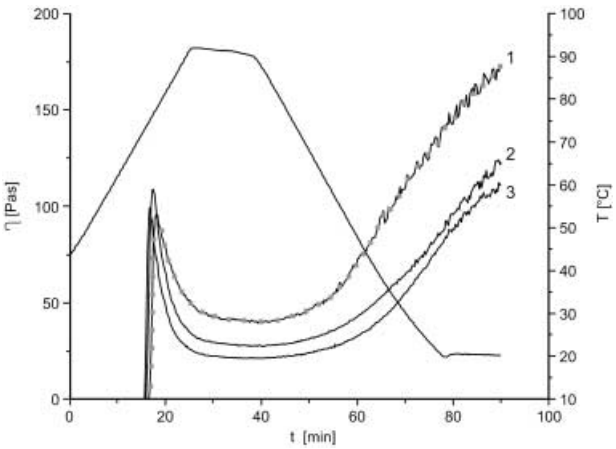

Figure 7 Viscosity profiles of KDIC15 (++) (1) and KDI20 (++) (2) starches compared to that of KD-UT (3).

Table 2 Overview of physicochemical properties and starch content of KDIC transformants. For description, see Table 1

Transformants	d_{50} (μM)	T_o (°C)	ΔH (kJ/g)	Amylose content (%)	Starch content (mg/g FW)
KD-UT	21.4 (± 0.7)	66.6 (± 0.3)	14.9 (± 1.0)	19.5 (± 0.4)	190.7 (± 15.2)
KDIC1 (–)	20.5 (± 0.6)	67.1 (± 0.2)	15.6 (± 1.6)	19.5 (± 0.2)	173.9 (± 16.7)
KDIC27 (–)	18.5 (± 0.3)	66.9 (± 0.1)	15.2 (± 0.8)	19.1 (± 0.0)	161.2 (± 7.7)
KDIC22 (+)	31.1 (± 0.9)	68.0 (± 0.4)	14.8 (± 0.5)	20.4 (± 0.3)	173.0 (± 32.4)
KDIC24 (+)	23.4 (± 0.5)	70.2 (± 0.1)	15.5 (± 0.8)	18.6 (± 0.1)	163.1 (± 19.6)
KDIC14 (++)	22.7 (± 0.6)	65.4 (± 0.1)	14.9 (± 1.4)	20.0 (± 0.4)	114.5 (± 43.6)
KDIC15 (++)	20.2 (± 0.4)	67.2 (± 0.1)	13.6 (± 1.8)	19.7 (± 0.2)	81.3 (± 37.3)

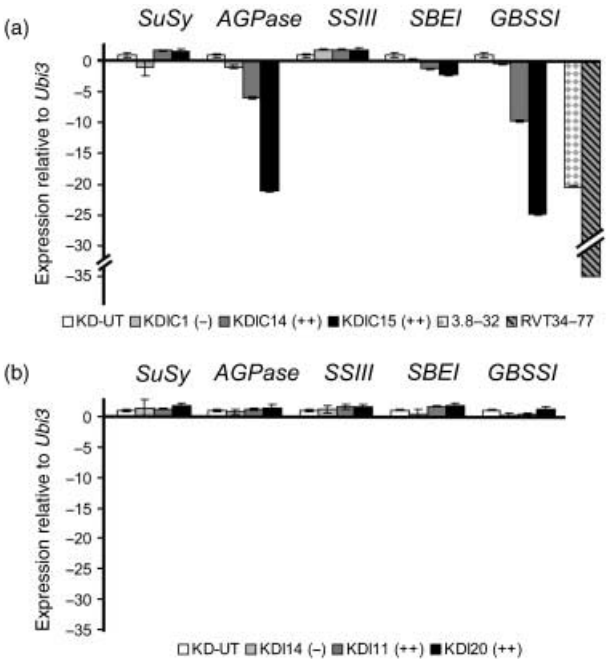

Figure 8 Real-time quantitative RT-PCR analysis of various KDIC (a) and KDI (b) transformants, and KD-UT tuber RNA. Expression levels of the following starch synthesizing genes were measured: *SuSy*, sucrose synthase; *AGPase*, ADP-glucose pyrophosphorylase subunit S; *SSIII*, starch synthase III; *SBEI*, starch branching enzyme I; *GBSSI*, granule-bound starch synthase I. RNA levels for each gene were expressed relative to the amount of *Ubi3* RNA, as described in materials and methods. RNA samples from Karnico potato tubers expressing a sense/antisense *GBSSI* cDNA construct exhibiting a partial (3.8–32) as well as a complete *GBSSI* down-regulation (RVT34-77), were used as positive controls (a).

no additional peaks were seen in the chain length distribution profile. After treatment of the debranched starches with α-amylase, the HPAEC profiles obtained with KD-UT and transgenic starches were identical. These data indicated that the mutan is predominantly present as a separate carbohydrate, which is not covalently attached to starch molecules. Summarizing, high *GtfICAT* gene expression seems to correlate with lower starch content and higher viscosity, in particular at the end of the gelatinization process.

Expression levels of AGPase and GBSSI are down – regulated in the (++) KDIC class

Real-time quantitative RT-PCR was performed to determine the expression level of key genes involved in starch biosynthesis (Kossmann and Lloyd, 2000) including sucrose synthase (*SuSy*), ADP-glucose pyrophosphorylase (*AGPase*), starch synthase III (*SSIII*), starch branching I (*SBEI*) and granule-bound starch synthase I (*GBSSI*) (Figure 8). Expression levels of *AGPase* and *GBSSI* were down-regulated in the (++) KDIC class when compared to the KDI transformants and KD-UT. For *GBSSI*, this down-regulation was quite similar to that of the 3.8–32 transformant in which *GBSSI* expression is partially inhibited. In contrast, this down-regulation was more than 20 times less than for the transformant RVT34-77 in which *GBSSI* is completely inhibited. Expression level of the *SBEI*, *SuSy* and *SSIII* genes in the (++) KDIC class remained unchanged. Concerning the KDI transformants, the expression levels of the different starch biosynthetic genes were comparable to that of KD-UT.

Discussion

This paper describes the production of mutan in potato tubers after expression of a full-length and a GBD-truncated *Gtf*I. *GtfICAT* expression led to a more efficient *in planta* production of mutan which was higher than expected, because *in vitro* experiments demonstrated that GTFICAT exhibited a lower activity (Monchois *et al*., 1999a). One reason for this could be that its transport to the amyloplast may be enhanced due to its decreased molecular weight. In addition, *GtfICAT* expression induced more severe developmental alterations in comparison to that of *Gtf*I, which were phenotypically visible at the tuber and starch levels. Tuber browning in the *GtfICAT*-expressing plants could be due to a stress response, probably resulting in the production of phenolic compounds (Tomás-Barberán and Espín, 2001). Interestingly, the link between tuber browning and production of foreign polymers in potato plants was reported previously (Pilon-Smits *et al*., 1996). In that study, a levansucrase gene with a vacuole-targeting sequence was expressed in potato tubers. Levansucrase and mutansucrase have in common that they consume sucrose, and consequently they can alter the sucrose pool size, and influence processes depending on sucrose. Because the vacuole contains approximately three times more sucrose than the amyloplast (Farré *et al*., 2001), vacuolar targeting of sucrose-converting enzymes may have a larger impact on plant development than plastidial targeting, at least when the activity of such enzymes is non-limiting. This is consistent with observations that the growth of levansucrase transformants was impaired, whereas that of mutansucrase transformants was not.

Sucrose conversion by GTFICAT may also induce changes at the gene transcription level. Supporting this, it was shown that the starch-synthesizing *AGPase* and *GBSSI* genes were down-regulated in KDIC transformants. These genes are known to be transcriptionally regulated by sucrose (Salehuzzaman *et al*., 1994; Geigenberger, 2003). *AGPase* down-regulation might explain the lower starch content of the KDIC transformants. However, the amylose content of these granules was similar to that of KD-UT granules, which seems to

disagree with their lower level of *GBSSI* transcript. This result differed from that of the 3.8–32 transformant in which the amylose content was lower, with an amount of *GBSSI* mRNA similar to that of the KDIC transformants. It needs to be mentioned that the down-regulation of *GBSSI* occurs in two different ways, at the transcriptional level for KDIC and at the post-transcriptional level for 3.8–32, respectively. Our result indicates that RNA degradation might affect the amylose content more severely than a less efficient transcription of the *GBSSI* gene.

Attachment of mutan to KDIC starch granules was not observed with KDI starch granules. To a certain extent, similar mechanisms may be at play in the attachment of mutan to starch granules and teeth surfaces. However, in the latter case, adhesion forces would be strengthened due to the synergistic action of various adhesive agents present in dental plaque (Balakrishnan *et al*., 2000). After exo-mutanase treatment, most of the mutan was detached from the starch granules and the remaining granule surfaces were comparable to those of KD-UT. Evidence for the presence of mutan inside starch granules was not found, although this possibility can not be excluded. Based on the chain length distribution experiments, it is not very likely that mutan is an intrinsic part of amylopectin and/or amylose molecules. The so-called acceptor reaction, which is poorly documented for GTFI, is apparently of minor importance inside the amyloplast. Furthermore, it is not known from the literature whether starch is a good acceptor molecule for mutansucrase. However, it is well-known that the acceptor reaction efficiency decreases substantially with increasing molecular weight of the acceptors (Kok-Jacon *et al*., 2003). Another explanation could be that the mutan concentration is too low in comparison to that of starch, thereby limiting the detection of attached mutan chains by HPAEC analysis.

Alterations in granule morphology were more severe for KDIC starches in which eroded and porous granules were commonly observed. Alterations in KDI starch granule morphology were also visualized despite the absence of stained mutan on starch granule surfaces upon erythrosine treatment.

Finally, mutan production in potato amyloplasts interfered with the rheological properties of the starches. The simultaneous presence of mutan and starch gave a higher viscosity after cooling the starch paste. It is possible that the mutans with their adhesive properties firmly interact with the amylopectin and amylose chains, thereby increasing the viscosity more than with a control starch, showing normal retrogradation.

This study is the first report dealing with the expression of a full-length and a GBD-truncated *Gtf*I gene in plants. Interestingly, it demonstrates that GTFICAT, which is still active after domain truncation, is an efficient catalyst for the enhanced production of foreign polymers in plants.

Experimental procedures

Preparation of constructs containing the mature and truncated *Gtf*I genes

An expression cassette containing the patatin promoter (Wenzler *et al*., 1989), the chloroplastic ferredoxin signal peptide (FD) from *Silene pratensis* (Pilon *et al*., 1995) fused to the NOS terminator was cloned into the pBluescript SK (pBS SK) plasmid, resulting in pPF. A mature mutansucrase (*Gtf*I) gene from *S. downei* Mfe28 (Ferretti *et al*., 1987; M17391) was ligated in frame between the signal peptide FD and the NOS terminator. The mature *Gtf*I gene was amplified by PCR, with a forward primer containing a *Sma*I restriction site (5′-AGCTTGCG-GCCCCGGGACTGAAAC-3′) and a reverse primer containing an *Eco*RI restriction site (5′-GTGGTGGTGGAATTCGAGT-TAGTTC-3′) using the proofreading *Pfu* turbo DNA polymerase (2.5 units/μL; Stratagene, UK) and cloned into the *SmaI*/*Eco*RI restriction sites of pPF, resulting in pPF*GtfI*. FD and the fused *Gtf*I gene were completely sequenced in one direction by Baseclear (the Netherlands) to verify the correctness of the construct. pPF*GtfI* was digested with *Xho*I and ligated into a pBIN20 binary vector (Hennegan and Danna, 1998), resulting in pPFI (Figure 1A).

For the construction of the FD-*GtfICAT*-NOS fusion, the mature *Gtf*I gene truncated at position 3150 was amplified by PCR, with a forward primer containing a *Sma*I restriction site (5′-AGCTTGCGGCCCCGGGACTGAAAC-3′) and a reverse primer containing an *Eco*RI restriction site (5′-AGAAGGAAT-TCTCATCTTAAACATTGAGGTA-3′) and cloned into the *SmaI*/*Eco*RI restriction sites of pPF, resulting in pPF*GtfICAT*. Sequencing and cloning into the pBIN20 binary vector, resulting in pPFIC (Figure 1B), were performed as for pPFI.

Transformation and regeneration of potato plants

pPFI and pPFIC were transformed into *Agrobacterium tumefaciens* strain LBA 4404 using electroporation (Takken *et al*., 2000). Internodal stem segments from the tetraploid potato genotype (cv. Kardal (KD)) were used for *Agrobacterium*-mediated transformation. Transformants were selected on plates with MS30 medium (Murashige and Skoog, 1962) containing kanamycin (100 mg/L). 30 transgenic, root forming, shoots were multiplied and five plants of each transgenic line were transferred to the greenhouse for tuber development. The mature tubers were harvested after 18 weeks.

Starch isolation

Potato tubers were peeled and homogenized in a Sanamat Rotor (Spangenberg, the Netherlands). The resulting homogenate was allowed to settle overnight at 4 °C. The starch pellet was washed three times with water and finally air-dried at room temperature for at least three days. The dried starch was powdered and stored at room temperature.

Expression analysis of *Gtf*I, *GtfICAT* and starch synthesizing genes using semi-quantitative and real-time quantitative RT-PCR analysis

RNA was isolated from 3 g (fresh weight) of potato tuber material from selected transgenic lines according to Kuipers *et al*. (1994).

For semi-quantitative RT-PCR, 50 μg of total RNA was treated with DNAseI and purified using the Gene-elute mammalian total RNA kit (Sigma, the Netherlands). The reverse transcription was performed using 5 μg of total RNA which was incubated for 5 min at 65 °C with 500 ng primer polydT (5′-TTTTTTTTTTTTTTTTTTTTTTTTT-3′) and 12.5 mM of each dNTP in a final volume of 12 μL. After centrifugation (30 s; 10 000 *g*), the mixture was incubated for 2 min at 42 °C with 4 μL of 5× first-strand buffer (Invitrogen, the Netherlands) and 2 μL of 0.1 M DTT. 1 μL of SuperScript II Rnase H^- reverse transcriptase (200 U/μL; Invitrogen) was added and the mixture was incubated for 50 min at 42 °C. Following this, the reaction was terminated by heating the sample for 15 min at 70 °C. 2.5 μL of cDNA was used in a standard PCR with the primer/Tm/cycle number combinations as described as below. For each combination, the cycle number was optimized in order to remain in the exponential phase of the PCR reaction. *GtfIRT* primers, 5′-CCGTGCTTACAGTACCTCAGC-3′ and 5′-GGTCGTTAGCATTGTAGGTGAAA-3′ (Tm = 59 °C, 35 cycles) were based on the *Gtf*I gene sequence (Ferretti *et al*., 1987). *Ubi3* primers, 5′-GTCAGGCCCAATTACGAAGA-3′ and 5′-AAGTTCCAGCACCGCACTC-3′ (Tm = 55 °C, 40 cycles) were used as an internal control and were based on the ubiquitin-ribosomal protein gene sequence (*Ubi3*) from potato (Garbarino and Belknap, 1994; L22576).

Expression levels of genes involved in starch biosynthesis were also determined in parallel by real-time quantitative RT-PCR and the corresponding primers were designed using the PRIMER EXPRESS software (version 1.5, PE Applied BioSystems, CA, USA): *SuSy* primers, 5′-GAGGACGTGGCAGGTGAAA-3′ and 5′-GGTACACTGTGTGACGCCCAT-3′ were based on the sucrose synthase mRNA sequence (Salanoubat and Belliard, 1987; AY205302). *AGPase* primers, 5′-GCTGGGACCCGACTTTATCC-3′ and 5′-CGGGAATGTCAATCAGACGAT-3′ were based on the ADP-glucose pyrophosphorylase subunit S mRNA sequence (Müller-Röber *et al*., 1990; X55155). *SSIII* primers, 5′-CACAGGAGGTGTCTGGAAACC-3′ and 5′-TGGAACTTGTGAAGGTGAGGC-3′ were based on the starch synthase III mRNA sequence (Marshall *et al*., 1996; X95759). *SBEI* primers, 5′-CCGAGCCCCACGAATCTAT-3′ and 5′-GGCTCAGAGCTGCTCATGC-3′ were based on the starch branching I enzyme mRNA sequence (Poulsen and Kreiberg, 1993; X69805). *GBSSI* primers, 5′-GAGCTTCTGGCAGTGAACCC-3′ and 5′-GGCAAGTGGAGCGATTTCTTC-3′ were based on the granule-bound starch synthase I gene sequence (van der Leij *et al*., 1991; X58453). *Ubi3* primers, 5′-TTCCGACACCATCGACAATGT-3′ and 5′-CGACCATCCTCAAGCTGCTT-3′ were used as an internal control as described previously. For real-time quantitative RT-PCR reactions, 1 μg of total RNA was treated with 0.5 μL DNAse I RNAse free (10 U/μL; Invitrogen) and incubated with 5 μL of 10 × *Taq*man RT buffer, 11 μL of 25 mM $MgCl_2$, 10 μL of 10 mM dNTP mix, 2.5 μL of 50 μM random hexamer primers, 1.0 μL RNAse inhibitor (20 U/μL) and H_2O until a final volume of 39 μL for 30 min at 37 °C and 5 min at 75 °C. For reverse transcription, the mixture was incubated 10 min at 25 °C and 30 min at 48 °C with 1 μL of MultiScribe reverse transcriptase (50 U/μL; Applied Biosystems). Following this, the reaction was terminated by heating the sample for 5 min at 95 °C. Aliquots of 50 ng of cDNA were used in SYBR-Green PCR according to the manufacturer's protocol on the ABI PRISM7700 sequence detection system (Perkin-Elmer, Applied Biosystems) with the primers mentioned above. Relative quantification of the target RNA expression level was performed using the comparative Ct method according to the User Bulletin #2 (ABI PRISM7700 sequence detection system, December 1997; Perkin-Elmer, Applied Biosystems). The Ct value is defined as the PCR cycle at which the amount of amplified target RNA reaches a fixed threshold. The differences in the Ct values, called ΔCt, between the target RNA and the endogenous *Ubi3* RNA were calculated in order to normalize the differences of cDNA concentrations present in each reaction. The differences in the ΔCt, called ΔΔCt, between a transformed and an untransformed potato plant were calculated in order to relate the target RNA expression level to that of untransformed plant. The target RNA expression level of transformed plants was calculated using the equation 2-EXP (ΔΔCt). The relative RNA expression is considered as significant when $-0.5 <$ relative RNA expression > 0.5. RNA samples from Karnico potato tubers expressing a sense/antisense GBSSI cDNA construct referred to as 3.8–32 and RVT34-77 (Heilersig *et al.* unpublished results) were used as positive control because it

is known that their *GBSSI* expression levels were partially and completely down-regulated, respectively.

Determination of morphological and physicochemical properties of starch granules

Analysis of starch granule morphology was performed by light microscopy (LM) (Axiophot, Germany) equipped with a Sony colour video camera (CCD-Iris/RGB) and scanning electron microscopy (SEM, JEOL 6300F, Japan). For LM, the granules were stained with a 2× diluted Lugol solution before visualization. For SEM, dried starch samples spread on silver tape and mounted on a brass disk were coated with a 20 nm platinum layer. Samples were then examined with a scanning electron microscope operating at an accelerating voltage of 1.5–3.5 keV. The working distance was 9 mm. Mutan polymers were visualized with LM by staining starch granules with a 10× diluted erythrosine red colouring agent (Disclosing Red-Cote solution) (American Dental Trading BV, the Netherlands). Mutan polymers and exo-mutanase were kindly provided by Dr A. Wiater (Department of Industrial Microbiology, Lublin, Poland). Mutan polymers were produced in presence of sucrose by a mixture of streptococcal glucosyltransferase (*Streptococcus mutans* 20381, *S. mutans* 6067 and *S. sobrinus* 6070) serving as a positive control (Wiater *et al*., 1999). Exo-mutanase (α 1,3-glucanase, EC 3.2.1.59) was produced by *Trichoderma harzianum* F-470 (Wiater and Szczodrak, 2002). Exo-mutanase treatments were performed with 25 mU of exo-mutanase enzyme in 0.2 M sodium acetate buffer (pH 5.5) at 40 °C for 48 h in presence of 10 mg (transgenic) starch. After brief centrifugation (1 min; 10 000 *g*), the supernatant was discarded and the starch granules were stained with the erythrosine red colouring solution.

Median values of the granule size distribution (d_{50}) were determined with a Coulter Multisizer II, equipped with an orifice tube of 200 μM (Beckman-Coulter, UK). Approximately 10 mg of starch was suspended in 160 mL Isoton II and the granule size distribution was subsequently measured by counting approximately 50 000 granules.

Gelatinization analysis was performed using a differential scanning calorimeter (DSC, Perkin-Elmer Pyris 1, the Netherlands) equipped with a Neslab RTE-140 cooling system. About 10 mg starch was weighed accurately into a stainless-steel pan and water was added until a starch moisture content of 20% was obtained. The pan was sealed and equilibrated overnight at room temperature before DSC analysis. The measurements were performed at a heating rate of 10 °C/min from 40 °C to 100 °C. Before use, the DSC was calibrated with indium and zinc, and an empty pan was used as a reference. The onset temperature of gelatinization (T_o) and the enthalpy (ΔH) were calculated automatically. The reported values are the average of three measurements.

Amylose content was determined as described by Hovenkamp-Hermelink *et al*. (1988). Starch was diluted in 50 μL $HClO_4$ (35%), followed by determination of the absorption at 618 nm and 550 nm after staining with Lugol solution.

For starch content determination, about 50 mg of potato tuber material was homogenized in 0.5 mL of 8 M HCl (25%). After adding 2 mL of DMSO, the samples were shaken for 1 h at 60 °C. Subsequently, 0.8 mL 5 M NaOH and 3.7 mL 0.1 M citric acid buffer pH 4.6 were added. After adjusting the volume to 10 mL with water, the samples were centrifuged for 10 min at 10 000 ***g***. 20 μL of supernatant were used for starch determination using the Boehringer kit (Boehringer, Germany) in a microplate reader (Bio-Rad 3550-UV). Calculations were performed using glucose released from a known amount of starch as a standard.

For determination of the chain length distribution, 5 mg of (transgenic) starch was suspended in 250 μL of DMSO and gelatinized for 15 min at 100 °C. After cooling down to room temperature, 700 μL of 50 mM NaAc buffer pH 4.0 was added. A sufficient amount of isoamylase (Hayashibara Biochemical Laboratories, Japan; 59 000 U/mg protein) to debranch the starch polymers completely was added to the mixture, which was incubated for 2 h at 40 °C. After inactivation of the enzyme for 10 min at 100 °C, 1 mL of 25% DMSO was added. For high-performance size-exclusion chromatography (HPSEC), 1 mL was used as such. For high-performance anion-exchange chromatography (HPAEC), the sample was diluted 5 times with a 25% DMSO solution. In parallel, undiluted isoamylase-treated samples were incubated with a sufficient amount of porcine pancreas α-amylase (Merck, Germany; 250 U/mg protein) to investigate whether contiguous α-(1 → 3) glucosyl residues linked to amylopectin side chains were present. After incubation for 3 h at 25 °C in 50 mM NaAc buffer pH 6.9 and inactivation of the enzyme for 10 min at 100 °C, 1 mL was used for HPAEC analysis.

HPSEC was performed on a P680 HPLC pump system (Dionex, USA) equipped with an ASI-100 automated sample injector (Dionex) and three TSKgel columns in series (a G3000 SWXL and two G2000 SWXL; 300 × 7.5 mm; Montgomeryville, USA) in combination with a TSKgel SWXL guard column (40 × 6 mm) at 35 °C. Aliquots of 100 μL were injected and eluted with 10 mM of NaAc buffer (pH 5.0) at a flow rate of 0.35 mL/min. The effluent was monitored using a RID-6 A refractometer (Shimatzu, Japan). This system was calibrated with dextran standards (10, 40, 70, 150, 250, 500 kDa; Pharmacia, Sweden). DIONEX CHROMELEON software version 6.50 SP4 Build

1000 was used for controlling the HPLC system and data processing.

In order to obtain a better separation of the smaller amylopectin side chains (in the range of 2–45 glucose residues), HPAEC was performed on a GP40 gradient pump system (Dionex) equipped with a CarboPac PA 100 column (4 × 250 mm; Dionex) at 35 °C. The flow rate was 1.0 mL/min and 20 μL sample was injected with a Dionex AS3500 automated sampler. Two eluents were used, eluent A (100 mM NaOH) and eluent B (1 M NaAc in 100 mM NaOH) as follows: 0 > 5 min (100% eluent B; rinsing phase); 5 > 20 min (100% eluent A; conditioning phase); 20 → 25 min (linear gradient 0–20% eluent B; 100–80% eluent A); 25 → 50 min (linear gradient 20–35% eluent B; 80–65% eluent A); 50 → 55 min (linear gradient 35–50% eluent B; 65–50% eluent A); 55 → 60 min (50% eluent B; 50% eluent A). The sample was injected at 20 min. The eluent was monitored by an ED40 electrochemical detector in the pulsed amperometric mode (Dionex).

Viscometric profiles from a 2% starch suspension were determined by applying a small oscillating shear deformation at a frequency of 1 Hz, using a Thermo Haake rheoscope. The rheometer was equipped with parallel plate geometry (typ C70/1 Ti) and the gap size was 0.1 mm. The pasting profile of the 2% starch-water (w/v) suspension was obtained by heating the suspension from 40 °C to 90 °C at a rate of 2 °C/min, where it was kept for 15 min followed by cooling to 20 °C at a rate of 2 °C/min. After this, the starch paste was held at 20 °C for 15 min. The Tg (start gelatinization temperature), Tp (peak temperature) and the corresponding viscosities were measured. Subsequently, the retrogradated sample was subjected to an amplitude sweep from 10 Pa to 1000 Pa within 60 s to check that the measurements were made in the linear region, in which the amplitudes of stress and strain are proportional to each other.

Acknowledgements

We would like to thank Isolde Pereira for her assistance with the tissue culture, Dirkjan Huigen for helping with the growth of the plants in the greenhouse and Ing. Jos Molthoff (PRI-WUR) for his assistance with SYBR-Green analysis. In addition, we are very grateful to Dr Adrian Wiater (Department of Industrial Microbiology, Lublin, Poland) for providing the mutan polymers and the mutanase enzyme.

References

Balakrishnan, M., Simmonds, R.S. and Tagg, J.R. (2000) Dental caries is a preventable infectious disease. *Aus. Dent. J.* **45**, 235–245.

Colby, S.M., McLaughlin, R.E., Ferretti, J.J. and Russell, R.R.B. (1999) Effect of inactivation of *gtf* genes on adherence of *Streptococcus downei*. *Oral Microbiol. Immunol*. **14**, 27–32.

Farré, E.M., Tiessen, A., Roessner, U., Geigenberger, P., Trethewey, R.N. and Willmitzer, L. (2001) Analysis of the compartmentation of glycolytic intermediates, nucleotides, sugars, organic acids, amino acids and sugar alcohols in potato tubers using a nonaqueous fractionation method. *Plant Physiol*. **127**, 685–700.

Ferretti, J.J., Gilpin, M.L. and Russell, R.R.B. (1987) Nucleotide sequence of a glucosyltransferase gene from *Streptococcus sobrinus* Mfe28. *J. Bacteriol*. **169**, 4271–4278.

Garbarino, J.E. and Belknap, W.R. (1994) Isolation of a ubiquitin-ribosomal protein gene (*ubi3*) from potato, and expression of its promoter in transgenic plants. *Plant Mol. Biol*. **24**, 119–127.

Geigenberger, P. (2003) Regulation of sucrose to starch conversion in growing potato tubers. *J. Exp. Bot*. **54**, 457–465.

Gerrits, N., Turk, S.C.H.J., van Dun, K.P.M., Hulleman, S.H.D., Visser, R.G.F., Weisbeek, P.J. and Smeekens, S.C.M. (2001) Sucrose metabolism in plastids. *Plant Physiol*. **125**, 926–934.

Haag, A.P., Maier, R.M., Combie, J. and Geesey, G.G. (2004) Bacterially derived biopolymers as wood adhesives. *Int. J. Adhesion Adhesives*, **24**, 495–502.

Hamada, S. and Slade, H.D. (1980) Biology, immunology, and cariogenicity of *Streptococcus mutans*. *Microbiol. Rev*. **44**, 331–384.

Hennegan, K.P. and Danna, K.J. (1998) pBIN20: an improved binary vector for *Agrobacterium*-mediated transformation. *Plant Mol. Biol. Report*, **16**, 129–131.

Hovenkamp-Hermelink, J.H.M., de Vries, J.N., Adamse, P., Jacobsen, E., Witholt, B. and Feenstra, W.J. (1988) Rapid estimation of the amylose/amylopectin ratio in small amount of tuber and leaf tissue of the potato. *Potato Res*. **31**, 241–246.

Kok-Jacon, G.A., Ji, Q., Vincken, J.-P. and Visser, R.G.F. (2003) Towards a more versatile α-glucan biosynthesis in plants. *J. Plant Physiol*. **160**, 765–777.

Kossmann, J. and Lloyd, J. (2000) Understanding and influencing starch biochemistry. *Crit Rev. Plant Sci*. **19**, 171–226.

Kuipers, A.G.J., Jacobsen, E. and Visser, R.G.F. (1994) Formation and deposition of amylose in the potato tuber starch granule are affected by the reduction of granule-bound starch synthase gene expression. *Plant Cell*, **6**, 43–52.

van der Leij, F.R., Visser, R.G.F., Ponstein, A.S., Jacobsen, E. and Feenstra, W.J. (1991) Sequence of the structural gene for granule-bound starch synthase of potato (*Solanum tuberosum* L.) and evidence for a single point deletion in the *amf* allele. *Mol. General Genet*. **228**, 240–248.

Leknes, K.N. and Lie, T. (1988) Erythrosin staining in clinical disclosure of plaque. *Quintessence Int*. **19**, 199–204.

Loesche, W.J. (1986) Role of *Streptococcus mutans* in human dental decay. *Microbiol. Rev*. **50**, 353–380.

Marchessault, R.H. and Deslandes, Y. (1980) Texture and crystal structure of fungal polysaccharides. *ACS Symp*, **126**, 221–250.

Marsh, P.D. (2003) Are dental diseases examples of ecological catastrophes? *Microbiol*. **149**, 279–294.

Marshall, J., Sidebottom, C., Debet, M., Martin, C., Smith, A.M. and Edwards, A. (1996) Identification of the major starch synthase in the soluble fraction of potato tubers. *Plant Cell*, **8**, 1121–1135.

Moire, L., Rezzonico, E. and Poirier, Y. (2003) Synthesis of novel biomaterials in plants. *J. Plant Physiol*. **160**, 831–839.

Monchois, V., Argüello-Morales, M. and Russell, R.R.B. (1999a) Isolation of an active catalytic core of *Streptococcus downei* Mfe28 Gtf-I glucosyltransferase. *J. Bacteriol*. **181**, 2290–2292.

Monchois, V., Willemot, R.M. and Monsan, P. (1999b) Glucansucrases: mechanism of action and structure-function relationships. *FEMS Microbiol. Rev*. **23**, 131–151.

Müller-Röber, B.T., Kossmann, J., Hannah, L.C., Willmitzer, L. and Sonnewald, U. (1990) One of two different ADP-glucose pyrophosphorylase genes from potato responds strongly to elevated levels of sucrose. *Mol. General Genet*. **224**, 136–146.

Murashige, T. and Skoog, F. (1962) A revised medium for rapid growth and bioassay with tobacco tissue culture. *Physiol. Plant*. **15**, 473–497.

Pilon, M., Wienk, H., Sips, W., de Swaaf, M., van't Talboom, I., Hof, R., de Korte-Kool, G., Demel, R., Weisbeek, P. and de Kruijff, B. (1995) Functional domains of the ferredoxin transit sequence involved in chloroplast import. *J. Biol. Chem*. **270**, 3882–3893.

Pilon-Smits, E.A.H., Ebskamp, M.J.M., Jeuken, M.J.W., van der Meer, I.M., Visser, R.G.F., Weisbeek, P. and Smeekens, S.C.M. (1996) Microbial fructan production in transgenic potato plants and tubers. *Ind. Crops Prod*. **5**, 35–46.

Poulsen, P. and Kreiberg, J.D. (1993) Starch branching enzyme cDNA from *Solanum tuberosum*. *Plant Physiol*. **102**, 1053–1054.

Robyt, J.F. (1995) Mechanisms in the glucansucrase synthesis of polysaccharides and oligosaccharides from sucrose. *Adv. Carbohydr. Chem. Biochem*. **51**, 133–168.

Russell, R.R.B., Gilpin, M.L., Mukasa, H. and Dougan, G. (1987) Characterization of glucosyltransferase expressed from a *Streptococcus sobrinus* gene cloned in *Escherichia coli*. *J. General Microbiol*. **133**, 935–944.

Salanoubat, M. and Belliard, G. (1987) Molecular cloning and sequencing of sucrose synthase cDNA from potato (*Solanum tuberosum* L.): preliminary characterization of sucrose synthase mRNA distribution. *Gene*, **60**, 47–56.

Salehuzzaman, S.N.I.M., Jacobsen, E. and Visser, R.G.F. (1994) Expression patterns of two starch biosynthetic genes in *in vitro* cultured cassava plants and their induction by sugars. *Plant Sci*. **98**, 53–62.

Sutherland, I.W. (2001) Biofilm exopolysaccharides: a strong and sticky framework. *Microbiol*. **147**, 3–9.

Takken, F.L.W., Luderer, R., Gabriëls, S.H.E.J., Westerink, N., Lu, R., de Wit, P.J.G.M. and Joosten, M.H.A.J. (2000) A functional cloning strategy, based on a binary PVX-expression vector, to isolate HR-inducing cDNAs of plant pathogens. *Plant J*. **24**, 275–283.

Tomás-Barberán, F.A. and Espín, J.C. (2001) Phenolic compounds and related enzymes as determinants of quality in fruits and vegetables. *J. Sci. Food Agric*. **81**, 853–876.

Tuohy, K.M., Probert, H.M., Smejkal, C.W. and Gibson, G.R. (2003) Using probiotics and prebiotics to improve gut health. *Drug Discovery Today*. **8**, 692–700.

Wenzler, H.C., Mignery, A., Fisher, L.M. and Park, W.D. (1989) Analysis of a chimeric class-I patatin-*GUS* gene in transgenic potato plants: High-level expression in tubers and sucrose-inducible expression in cultured leaf and stem explants. *Plant Mol. Biol*. **12**, 41–50.

Wiater, A., Choma, A. and Szczodrak, J. (1999) Insoluble glucans synthesized by cariogenic streptococci: a structural study. *J. Basic Microbiol*. **39**, 265–273.

Wiater, A. and Szczodrak, J. (2002) Selection of strain and optimization of mutanase production in submerged cultures of *Trichoderma harzianum. Acta Biol. Hung*. **53**, 389–401.

Wren, B.W. (1991) A family of clostridial and streptococcal ligand-binding proteins with conserved C-terminal repeat sequences. *Mol. Microbiol*. **5**, 797–803.